Electronic Supplementary Information (ESI)

Near-infrared luminescence and high thermal stability of $Rb_2NaScF_6:Cr^{3+}$ phosphor for spectroscopy applications

Lingxiang Chu, Yi Qin, Tao Yang, Jing Wan, Qiang Zhou,* Huaijun Tang, Yanqing Ye, Zhengliang Wang*

Key Laboratory of Green Chemistry Materials in University of Yunnan Province, Key Laboratory of Advanced Synthetic Chemistry (Yunnan Minzu University) of National Ethnic Affairs Commission, School of Chemistry and Environment, Yunnan Minzu University, Kunming 650500, P. R. China.

Corresponding Author:

*Email: q-zhou@ymu.edu.cn (Q. Zhou)

wangzhengliang@foxmail.com (Z. Wang)

The NIR emission can be verified by calculating the ratio of Dq/B for the estimation of crystal field strength surrounding Cr^{3+} ion being weak or strong with a dividing point of 2.3. The local crystal field strength Dq and the related parameter B can be calculated according to the following equations:[S1]

$$10Dq = E\left({}^4T_2\right) = E\left({}^4A_2 \rightarrow {}^4T_2\right)$$

$$\frac{Dq}{B} = \frac{15\left(\Delta E/Dq - 8\right)}{\left(\Delta E/Dq\right)^2 - 10(\Delta E/Dq)}$$

where ΔE means the energy difference between $^4T_2$ and $^4T_1$ levels, which can be obtained from the PLE peak energies of $^4T_1$ (22831 cm^{-1}) and $^4T_2$ (15528 cm^{-1}) levels. The Dq, B and Dq/B values calculated according to the above formula are 1552 cm^{-1}, 782 cm^{-1} and 1.98, illustrating Cr^{3+} ions undergo a weak crystal field in RNSF host.

To further explain the concentration quenching mechanism, the following formula was adopted to calculate the critical distance R_c among adjacent Cr^{3+} ions:[S2]

$$R_c \approx 2\left(\frac{3V}{4\pi x_c N}\right)^{1/3}$$

where N is the site number that can be replaced by Cr^{3+} in each unit cell. V and x_c represent unit cell volume and doping concentration. Based on the refinement result of RNSF:0.03Cr, V = 637.9565 Å, x_c = 0.03, N = 4, R_c is calculated to be 21.66 Å, which is about four times larger than the exchange interaction value (5 Å), indicating that the non-radiative relaxation is assignable to the multipole interaction.

According to Dexter theory, the main type of multipolar interaction can be evaluated *via* the following equation:[S3, S4]

$$\frac{I}{x} = K\left[1 + \beta(x)^{\theta/3}\right]^{-1}$$

Here, I and x are the emission intensity and Cr^{3+} dopant concentration, respectively. K and β are the known constants. By plotting the relationship between $\log(I/x)$ and $\log(x)$, a linear fitting curve with a slope of -0.841 and a reliable correlation coefficient of 0.9957 is obtained, and the calculated θ value is 2.523, which is close to 3. This result strongly indicates that the energy transfer between the nearest or next nearest Cr^{3+} ions is the main reason for the concentration quenching of Cr^{3+} in RNSF host.

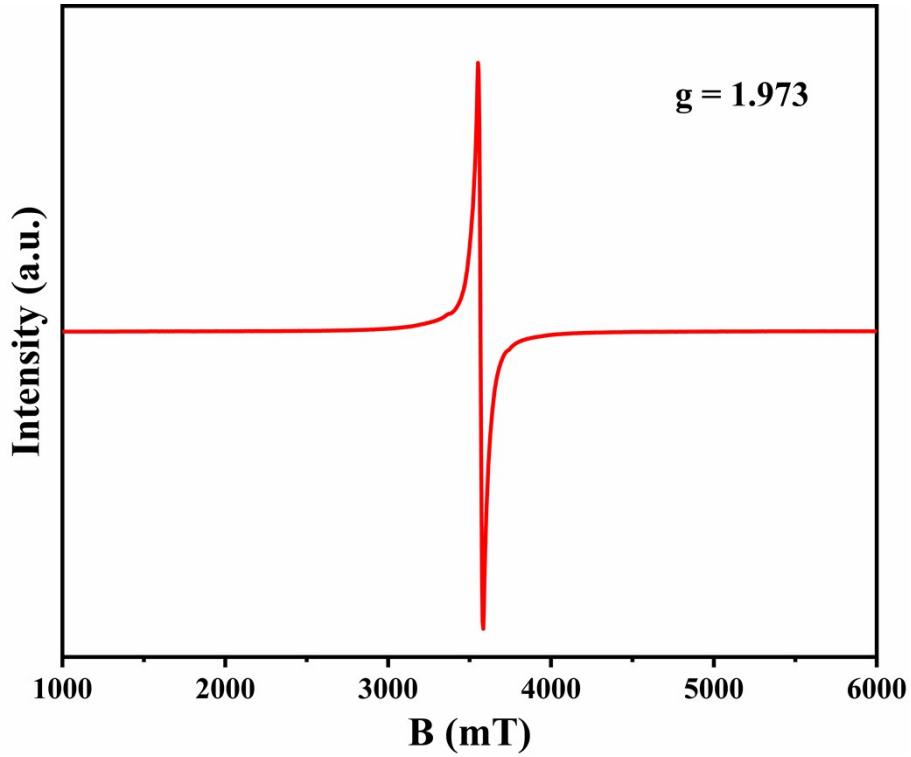

Fig. S1. EPR spectrum of RNSF:Cr.

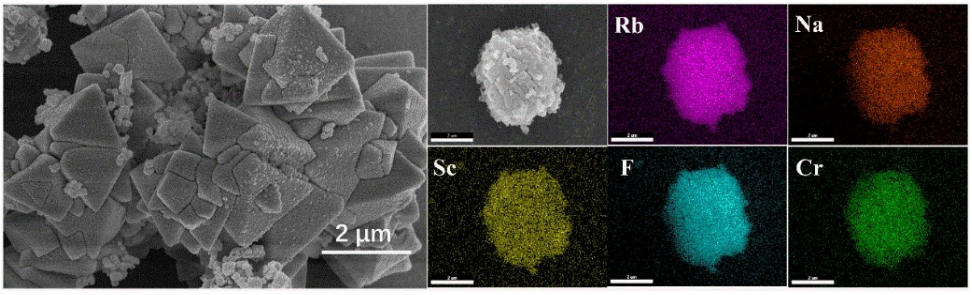

Fig. S2. SEM and elemental mapping images of RNSF:Cr product.

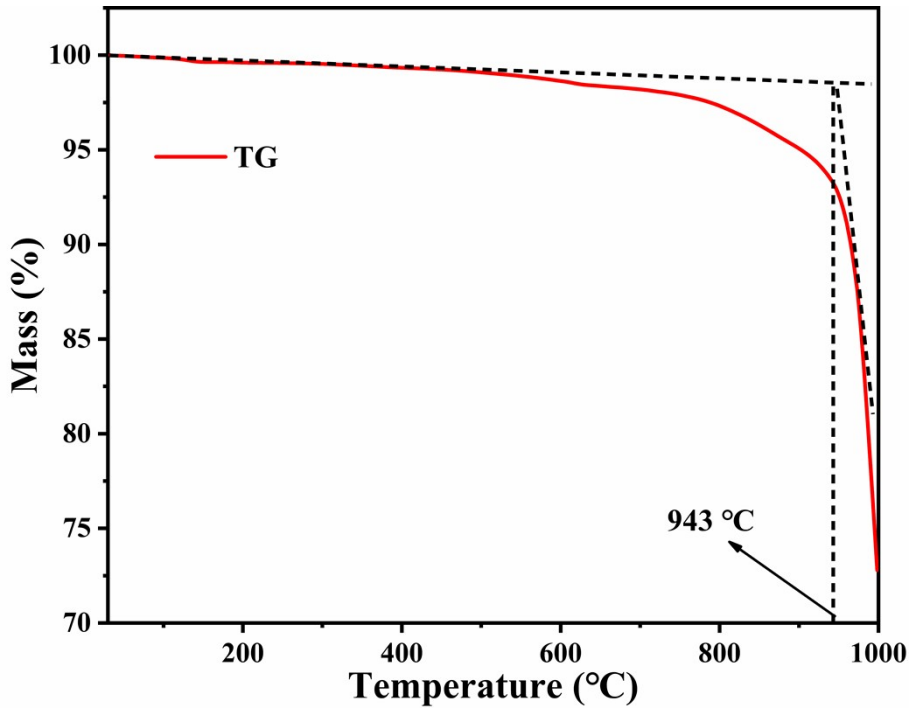

Fig. S3. TG curve of RNSF:Cr phosphor.

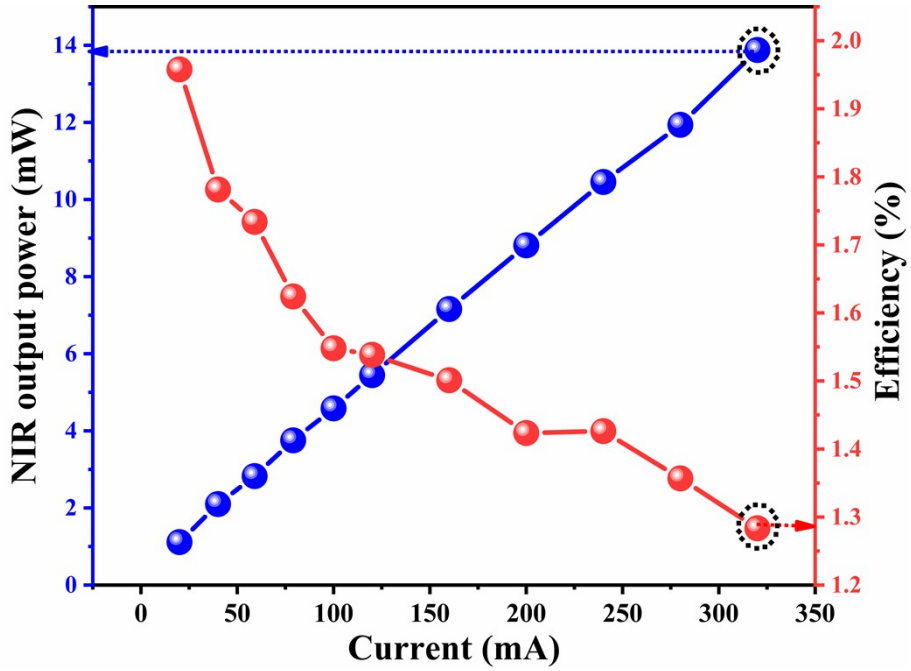

Fig. S4. NIR output power and photoelectric conversion efficiency of pc-LED device ranging from 20 to 320 mA.

Table S1. The crystallographic parameters of RNSF host and RNSF:0.03Cr sample.

Formula	RNSF	RNSF:0.03Cr
Crystal system	Cubic	Cubic
Space group	$Fm\bar{3}m$	$Fm\bar{3}m$
Space group number	225	225
a (Å)	8.6098	8.6085
b (Å)	8.6098	8.6085
c (Å)	8.6098	8.6085
α	90.0000	90.0000
β	90.0000	90.0000
γ	90.0000	90.0000
V (Å^3)	638.2544	637.9565
Z	4	4
R_{wp} (%)	7.83%	7.28%
R_p(%)	5.43%	5.07%
χ^2	1.992	1.978

Table S2. Photoluminescence properties of the Cr^{3+}-activated fluoride NIR-emitting phosphors.

Phosphor	λ_{em} (nm)	$I_{150°C}$ (%)	Ref.
$K_2NaScF_6:Cr^{3+}$	765	89.6	[S5]
$K_2NaAlF_6:Cr^{3+}$	728	96.5	[S6]
$K_2NaGaF_6:Cr^{3+}$	748	82.1	[S6]
$K_2NaInF_6:Cr^{3+}$	774	78.3	[S6]
$Cs_2KGaF_6:Cr^{3+}$	782	88.7	[S7]
$Cs_2KAlF_6:Cr^{3+}$	755	90.2	[S8]
$Rb_2KAlF_6:Cr^{3+}$	745	95.3	[S8]
$Na_3AlF_6:Cr^{3+}$	720	70	[S9]
$K_3Al/GaF_6:Cr^{3+}$	750	33	[S10]
$LiCaAlF_6:Cr^{3+}$	764	66.63	[S11]
$LiSrAlF_6:Cr^{3+}$	820	55.47	[S11]
$NaSbF_4:Cr^{3+}$	760	56.7	[S12]
$Rb_2NaScF_6:Cr^{3+}$	775	92	This work

Reference:

[S1] S. Adachi, *J. Lumin.*, 2021, **232**, 117844.

[S2] Y. Chen, F. Liu, Z. Zhang, J. Hong, M.S. Molokeev, I.A. Bobrikov, J. Shi, J. Zhou, M. Wu, *J. Mater. Chem. C*, 2022, **10**, 7049–7057.

[S3] J. Chen, C. Guo, Z. Yang, T. Li, J. Zhao, *J. Am. Ceram. Soc.*, 2016, **99**, 218–225.

[S4] L. You, R. Tian, T. Zhou, R. J. Xie, *Chem. Eng. J.*, 2021, **417**, 129224.

[S5] E. Song, H. Ming, Y. Zhou, F. He, J. Wu, Z. Xia, Q. Zhang, *Laser Photonics Rev.*, 2021, **15**, 2000410.

[S6] J. Li, H. Zhe, H. Ming, Y. Zhou, Y. Ye, Q. Zhou, Z. Wang, *Mater. Today Chem.*, 2022, **24**, 100839.

[S7] Z. Wu, X. Han, J. Wang, Y. Zhou, K. Xing, S. Cao, J. Zhao, B. Zou, R. Zeng, *J. Mater. Chem. C*, 2022, **10**, 10292-10301.

[S8] Q. Fan, J. Li, J. Yang, Y. Zhou, Q. Zhou, Z. Wang, *Mater. Res. Bull.*, 2023, **158**, 112065.

[S9] D. Yu, Y. Zhou, C. Ma, J. H. Melman, K. M. Baroudi, M. LaCapra, R. E. Riman, *ACS Appl. Electron. Mater.*, 2019, **1**, 2325–2333.

[S10] C. Lee, Z. Bao, M. H. Fang, T. Lesniewski, S. Mahlik, M. Grinberg, G. Leniec, S. M. Kaczmarek, M. G. Brik, Y. T. Tsai, T. L. Tsai, R. S. Liu, *Inorg. Chem.*, 2020, **59**, 376–385.

[S11] D. Wu, L. Liu, H. Liang, H. Duan, W. Nie, J. Wang, J. Peng, X. Ye, *Ceram. Int.*, 2022, **48**, 387–396.

[S12] X. Zhang, K. Chen, T. Deng, J. Yuan, R. Zhou, T. Yu, Y. Zhou, E. Song, *Mater. Today Chem.*, 2022, **26**, 101194.